CrystEngComm

Accepted Manuscript

ROYAL SOCIETY OF CHEMISTRY

www.rsc.org/crystengcomm

Journal Name

ARTICLE

Experimental evidences of ZnS precursors anisotropy activated by ethylenediamine for constructing nanowires and single atomic layered hybrid structure

Received 00th January 20xx,
Accepted 00th January 20xx

DOI: 10.1039/x0xx00000x

www.rsc.org/

Shaobo Han,[ab] Wei Liu,*[a] Kai Sun[b] and Xiaotao Zu*[c]

Size and phase-controlled growth and assembly of semiconductor nanostructures from ultrasmall building blocks is of great significance in aspects of both science and engineering. In this work, ZnS nanostructures including nanoparticles, nanobelts, single-crystal nanowires and layered $ZnS(EN)_{0.5}$ hybrid structure are flexibly synthesized in one-pot solvothermal system using ethylenediamine (EN) as the sole coordination agent. Comprehensive structure characterizations, especailly including the spherical abberation corrected STEM imaging under ultralow current density ($2.55A/cm^2$), provide direct evidences that role of EN molecules varies from surface stabilizer to internal bridging blocks with changing the introduction opportunities. When introduced after the formation of ZnS precursors, EN passivates the none-polarized facets of ZnS clusters and activates the anisotropic growth along the [001] axes of the ZnS clusters into either 1D wurtzite nanowires. When it is added before the formation of the ZnS clusters, EN serves as the bridging blocks yielding layered $ZnS(EN)_{0.5}$ hybrid structures through the connection of wurtzite ZnS (110) slabs. The layered $ZnS(EN)_{0.5}$ nanostructures turn into single-crystal nanobelts after the removal of the EN components.

Introduction

In the last few years, much attention has been focused on the synthesis and construction of semiconductor nanomaterials to control their unique properties. As one representative direct band-gap semiconductor, ZnS has been extensively investigated benefiting for its potential applications in electronics, optics, biomedicine, and mechanics.[1-7] Indeed various structures such as 1-dimension (1D, nanotubes, wire, rods, belts and ribbons)[8-10], 2-dimensional (2D, sheet, platelets and diskettes)[11-13] and 3-dimensional (3D, tetrapod and hierarchical)[14-16] have been prepared through different methods such as irradiation, solvothermal, chemical vapor deposition and so on. Of particular interest is the employ of solvothermal methods for size and form-controlled synthesis of ZnS nanostructures that usually uses organic amine molecules to modulate the growth in the tetrahedrally coordinated structure. Ethylenediamine (EN) has been widely used as ligand for the construction of metal-organic frameworks. This capping ligand imposes both the 1D nature of the substructure and the local coordination at the metal sites, organizing these substructures in a periodic and regular fashion within the crystals via the nonsulfur bridging functions.[17-18] Various chalcogenide lamellar phases of inorganic–organic hybrids have been synthesized using EN as the ligand demonstrating its feasibility to be intercalated in ZnM (S, Se, Te) sheets.[19-21] Acharya et al. recently reported that the layered structure of ZnS transforms from zinc blend to wurtzite with the change of the EN concentration.[22] Such configurations denoted as $M(EN)_{0.5}$ with EN as bridging molecules have been frequently reported in diverse II-VI nanostructures.[23] However, to our best knowledge, direct microscopy imaging evidences has never been provided except some X-ray diffraction (XRD) results. In our previous work, ZnS nanoparticles (NPs),[24] ultrathin nanobelts (NBs),[25] and branched nanotetrapods (TPs),[26] were successively obtained through controlling the EN concentration. While deep insights still need to be put forward into the delicate steps of crystal growth and the pathway for development of diverse configurations on the basis of all the reported ZnS products.

In the present study, we perform an elaborate investigation on the modulation effect of EN molecules on the growth of diverse ZnS based nanostructures including NPs, NWs, $ZnS(EN)_{0.5}$ hybrid structures and single-crystal NBs. Experimental evidences from comprehensive characterizations, including powder XRD patterns, high resolution transmission electron microscopy (HRTEM), UV-vis absorption spectroscopy, and fourier transform infrared spectroscopy (FTIR) disclose the interaction details between the EN molecule and the ZnS crystals, shedding lights on the growing details of all the ZnS

[a] School of Physical Electronics, University of Electronic Science and Technology of China, Chengdu 610054, China. E-mail: weiliu@uestc.edu.cn
[b] Department of Materials Science and Engineering, University of Michigan, Ann Arbor, MI 48109, USA.
[c] Institute of Fundmental and Frontier Sciences, University of Electronic Science and Technology of China, Sichuan, Chengdu, 610054, China. E-mail: xtzu@uestc.edu.cn
*Corresponding author: weiliu@uestc.edu.cn (Liu); xtzu@uestc.edu.cn (Zu).

products, varying from 1D to 3D and zinc blende (ZB) to wurtzite (WZ).

Experimental

Materials and Preparation

All chemicals used with chemically pure grade were purchased without further purification. In a typical procedure, $Na_2S•9H_2O$, $Zn(Ac)_2•2H_2O$ and EN were used as the main reactants in the ethylene glycol (EG) solvothermal system. Initially, 0.2M $Na_2S•9H_2O$-EG and 0.1M $Zn(Ac)_2•2H_2O$-EG solution were prepared, respectively; then reactions were initiated following three schemes below, (a) 10mL Na_2S-EG solution and 10mL $Zn(Ac)_2$-EG solution, (b) 10mL Na_2S-EG solution, 10mL $Zn(Ac)_2$-EG solution and 30 mL EN and (c) 10mL Na_2S-EG solution, 30 mL EN and 10mL $Zn(Ac)_2$-EG solution were added into three 100mL volume autoclaves, and the total solution volume was kept as 65 mL by adjusting EG. After stirring and ultrasonic mixing for 30 min, the autoclaves were heated and kept at 180°C for 15h and cooled to ambient temperature naturally. The products (a) ZnS nanoparticles (NPs), (b) ZnS nanowires (NWs) and (c) $ZnS(EN)_{0.5}$ nanobelts (NBs) were collected and washed with the alcohol and distilled water for at least 3 times each. Then, the sample C was subject to additional reaction, where it was added into 100 mL volume autoclave containing 65mL EG, sealed and kept at 180°C for 5h and then cooled to room temperature. The resulting white precipitate ZnS NBs with distilled water and absolute ethanol.

Characterization

The microstructures of the synthesized nanomaterials were characterized by transmission electron microscopy (TEM, FEI Tecnai F30) and scanning transmission electron microscopy (STEM, JEOL 3100R05 cold emission Cs-corrected). XRD (DX-2700, Cu/K-alpha1) characterizations were conducted to identify the phase of the ZnS products. UV – vis measurement was carried out on a UV–vis spectrophotometer (Shimadzu UV–2500) at room temperature. FTIR spectra were recorded in the range 400–4000 cm-1 employing a Perkin-Elmer spectrometer by KBr pellet method in order to study the metal complex coordination.

Results and discussion

XRD characterizations were conducted firstly to study the basic structures of the as prepared ZnS nanomaterials. The XRD pattern taken from sample A can be indexed to be zinc blende phase (PDF#05-0566). However, the XRD pattern of the sample $ZnS(EN)_{0.5}$ nanobelts can neither indexed to zinc blende nor wurtzite. It matches that described by Ouyang et al.[27] and the strongest reflection at 2θ=10.2° (d=8.67 Å) is in good agreement with the interlayer spacing between the wurtzite ZnS sheets described as $ZnS(EN)_{0.5}$. Such a layered microstructure is constructed by inserting EN monolayers into the (110) planes of WZ ZnS phase. Figure 1(b) and (d) illustrate the XRD patterns from sample B and sample D respectively, which all correspond to the wurtzite phase ZnS (PDF#36-1450). It is also noted that the reflection peaks of sample D are much sharper than those of sample B. This difference could be attributed to either the better crystallinity of sample D or the smaller crystal size of sample B. The peak about 10 deg is results from the distance between NWs which are connected by ethylenediamine molecules. Further evidence on this point will be provided by the TEM results. Besides, the comparison of XRD pattern (c) and (d) reveals that the additional solvothermal reaction has reconstructed the structure from layered $ZnS(EN)_{0.5}$ to pure wurtzite phase ZnS. The phase diversity confirmed by XRD results indicates that microstructures of ZnS not only evolve with the EN concentration but also vary with the adding sequences of reagents.

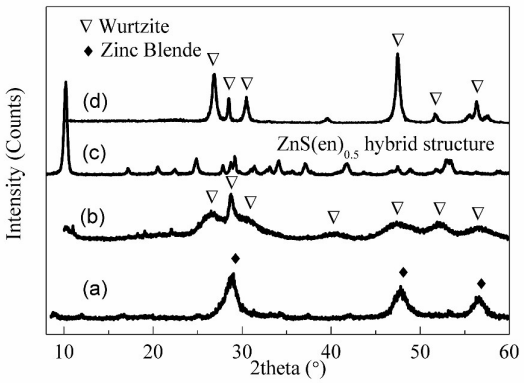

Fig. 1 XRD patterns taken from the as-synthesized (a) ZnS (NPs), (b) ZnS (NWs), (c) $ZnS(EN)_{0.5}$ hybrid structure and (d) ZnS NBs samples

When increase the EN concentration, it turns to transform from cubic to hexagonal. While changing the addition opportunity of EN, it brings significant impact on both configuration and crystallinity of ZnS products ascribed to the surface passivation and spacing effect of EN molecules.

The as prepared four kinds of ZnS products are divided into two comparison groups in the following TEM study in order to figure out the detailed information of the modulation effect of EN. In the first group, the morphologies and microstructures of sample A and B are shown in Fig. 2. The sample A is composed of ZnS NPs with average diameter of 6~8nm with no EN introduced (Fig.2a and c). Figure 2b gives the HRTEM image of two hexagon-shaped ZnS crystals, the two zinc blende nanocrystals are connected together by sharing {111} facets. This indicates that the ZnS NPs prefer to growth even at absence of EN. On the contrast, when 30 mL EN is introduced, ZnS NWs of high uniformity and large aspect ratio are obtained as shown in Fig. 2d. The NWs are in average length of ~1μm and diameter of ~2 nm, and also they are prefer to linked together along the side due to the absorption of ethylenediamine molecules. Figure 2e and 2f show two different conditions, one is that two nano-wires connected by {110} facets and the other is {100} facets(as shown in the inserted FFT images, respectively).

The above evidences manifest a remarkable modulation effect of EN on microstructure as well as the growth behavior of ZnS materials. It changes the atoms stacking sequences of primarily formed ZnS clusters from ZB phase (ABCABC sequence) to WZ phase (ABAB sequence) and meanwhile activating the anisotropic growth along the [001] axis of WZ into 1D structure.

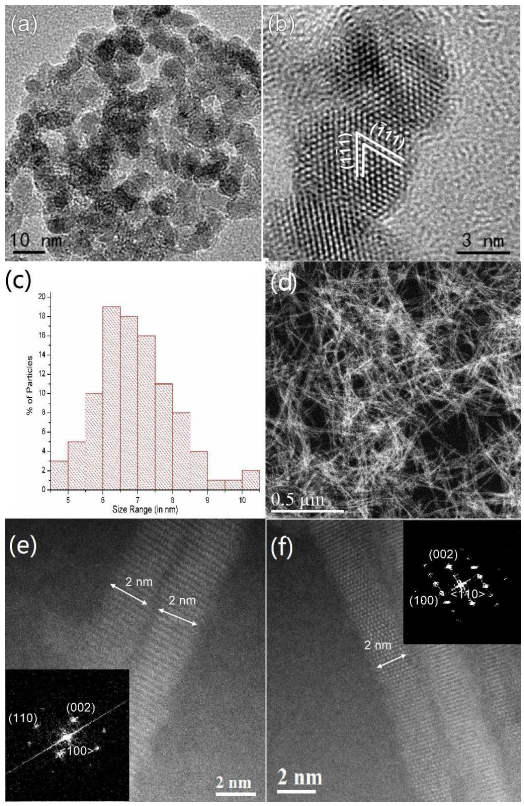

Fig. 2 High magnified and high-resolution TEM/STEM images demonstrating the nanoparticles morphology of sample A (a~b) and nanowires morphology of sample B (d~f); (c) Size distribution of the ZnS NPs.

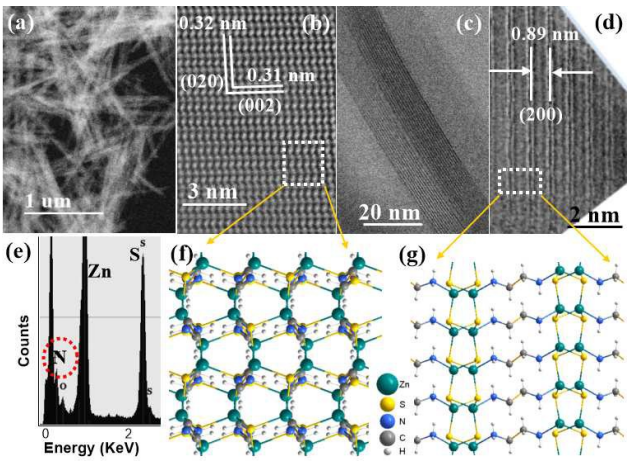

Fig. 3 (a, b, c and d) low magnified and high-resolution BF-STEM images of $ZnS(EN)_{0.5}$ NBs; (e) the corresponding EDX spectra; (f and g) schematic diagrams of $ZnS(EN)_{0.5}$ layered structure as viewed in [100] and [010] directions respectively.

Figure 3 demonstrates the TEM analysis of $ZnS(EN)_{0.5}$ NBs and ZnS NBs as the second comparison group for elucidating the modulation effect of EN. Different from the former situation where EN does not participate in the construction of ZnS nanostructure, layered $ZnS(EN)_{0.5}$ structure has been obtained as revealed by the XRD resutls. Figure 3(b, c and d) show the TEM as well as the high resolution STEM images of $ZnS(EN)_{0.5}$ inorganic-organic hybrid structure. Fig. 3b shows the HREM image with zone axis <200>, the distance 0.32nm and 0.31nm corresponding to lattice planes (020) and (002). The EN molecules serve as the bridging blocks between every two (110) WZ ZnS slabs through connecting Zn atoms and the $–NH_2$ at the tips of EN molecule by sharing the lone pair electrons, and the distinct interplanar distance is measured to be 0.89nm as shown in Fig. 3c and d, which coincides precisely with predict value of (200) lattice plane based on the XRD measurement. To the best knowledge of us, it has been the first time to obtain the high resolution microscopy evidence on kinds of $ZnS(EN)_{0.5}$ hybrid structure. The EDS spectrum in Fig. 3e shows that the as-fabricated NBs are composed of Zn, S and N elements without other impurities. The peak of nitrogen element further confirms the formtion of $ZnS(EN)_{0.5}$ hybrid structure.

Figure 4a show TEM image of the ZnS NBs which obtained from the additional solvothermal treatment of $ZnS(EN)_{0.5}$ NBs. SAED patterns corresponding to the ZnS NBs front and side respectively (as shown in Fig. 4b and c), coincide with WZ ZnS <110> and <100> zone axis. This results further confirmed that the layered $ZnS(EN)_{0.5}$ structure is constructed by (110) WZ ZnS slabs. Different from the EDS pattern in Fig. 3e, no N peak shows up in Fig. 4d, which reveals that EN molecules have been removed from the $ZnS(EN)_{0.5}$ NBs.

The EN modulation effect on ZnS phases have been further attested by FTIR and Uv-vis results as demonstrated in Fig. 5. Remarkable differences of optical absorption behaviors reflect distinct interactions between EN molecules and diverse ZnS nanostructures. Spectrum d in Fig. 5A shows the EN IR spectra in pure liquid state presenting broad and strong vibrations bands. However, when EN forms a complex with metal ions [$ZnS(EN)_{0.5}$] (spectrum b in Fig. 4A), the stretching vibration band of the N–H at frequency above 3240 cm-1 shifts to lower Besides, at frequencies below 1200 cm-1, the IR spectra of $ZnS(EN)_{0.5}$ exhibit many differences from the pure EN, which should be ascribed to the ordered alignment of EN molecules as the conformation of the EN molecules are randomized due to thermal perturbation in liquid-state. After the additional solvothermal treatment at 180 °C (spectrum a in Fig. 5A), the weaker vibration bands of the $ZnS(EN)_{0.5}$ hybrid suggests that it decomposes to form ZnS.[28,29] Compared with ZnS(EN)0.5, the ZnS NWs maintained the same typical vibrations of pure EN (spectrum c in Fig. 5A, indicating weaker interactions and disordered arrangements of few EN molecules absorbing on the surface.

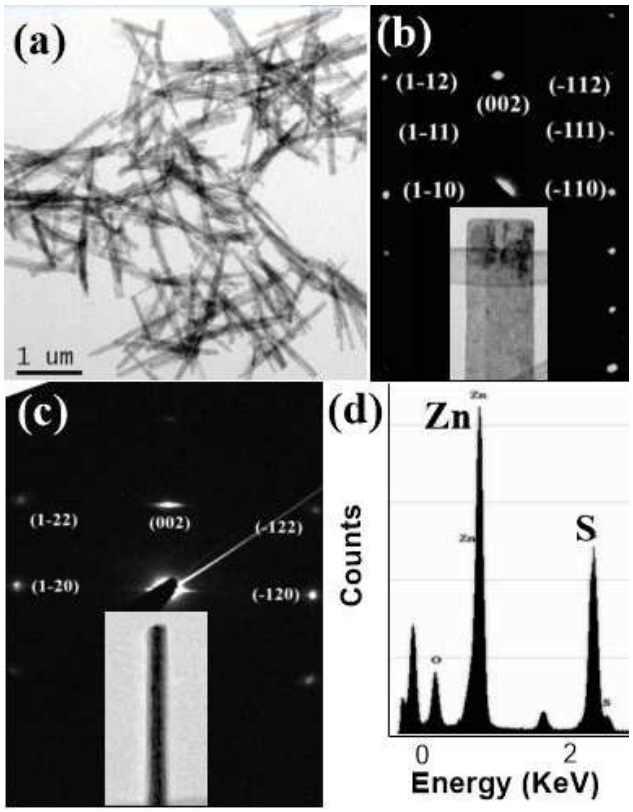

Fig. 4 (a) low magnified TEM image of ZnS NBs; (b, c) SAED patterns from the anterior and lateral orientations, respectively (as shown in the inserted images); (d) the corresponding EDX spectra.

UV-vis absorption results in Fig. 5B and 5C reveal band structures of high flexibility for diverse ZnS nanostructures. The optical absorption in the edge region can be well-fitted to produce the band gap value for direct band semiconductors[30]as shown in the insert figures. In Fig. 5B, the absorption curves of precursor and corresponding products have similar peaks, corresponding to the band gap of 4.4eV and 3.92eV respectively. This can be ascribed to the better crystallinity and quantum confinement effect.[31,32]ensity of this peak increased significantly after the formation of layered $ZnS(EN)_{0.5}$ hybrid structure and ZnS NWs as marked by the arrow. This fact indicates that the final products shall form via self-assembly of two different of ultra-small building blocks (a kind of ZnS-EN hybrid clusters). Yao et al. reported that pure $ZnS(DETA)_{1/2}$ shows a sharp absorption peak at 260 nm.[33] Fang et al. also observed such peak in ZnS nanobelts synthesized via chemical vapour deposition method.[34] These results reveal that this peak does not arise from organic molecules since no EN was used in their approaches. Rebilly et al. attributed it to the low dimensionality of the metal-sulfur arrangement.[35] Furthermore, the absorption curve of the ZnS NBs shows no peak at 263 nm, which coincides with its single crystal structure without EN inside. In Fig. 5C, the band gap of ZnS NPs and NBs are 3.60 eV and 3.51eV which are smaller than the bulk ZnS materials 3.68eV. A red-shift absorption can be observed compared to the precursor absorption peak at 285 nm. This could be attributed to the particles size increased and defect levels caused by collapse of $ZnS(EN)_{0.5}$ layered structure due to the remove of the EN molecules.

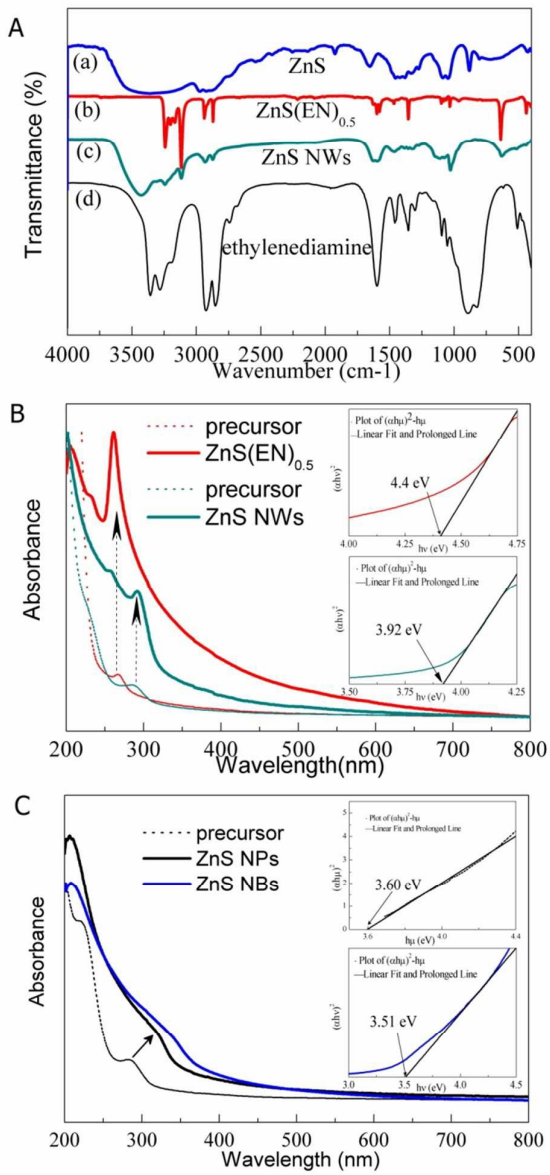

Fig. 5 A. FTIR spectra and UV-vis absorption spectra; (B and C) the as-prepared ZnS samples.

The above evidences disclose different roles of EN on the growth of ZnS NWs and $ZnS(EN)_{0.5}$ NBs varying from surface stabilizer to direct building blocks, the adding opportunities make significant selections among these roles. For decades, inorganic nanoparticles are known to self-assemble into lager structure through growth process.[36-40] Tang et al. have reported oriented self-organization of CdTe or Cu_2S NPs into NWs by strong long-range interactions.[41,42] In their experiment, one of the key steps was removal of excess stabilizer from the surface of CdTe colloids to activate the oriented self-organization. On the contrast in our schemes, it is the utilization of EN as stabilizer that initiates the anisotropic

growth of 1D nanostructures. Specially, when there is no EN, connection between ZnS NPs is messy and there is no fixed direction. When moderation amount of EN (30mL) is added, nanoclusters surface is passivated by EN molecules except the polarized (001) facets, and then the ZnS NPs oriented attachment along the [001] direction. Therefore, by a combination of self-assembly and oriented attachment growth, the crystal growth along the [001] direction lead to the formation of one-dimensional NWs. This is supported by another evidence implied in Fig. 2. The characteristic size (~2nm) is maintained during EN modulated transformation from NPs to NWs, which could be ascribed to scale-related modulation effect of EN. It means that if EN is introduced after the formation of ZnS clusters (scheme B), it prefers to modulate the crystal growth behavior at lattice scale rather than the assembly manner at nanoscale. However, when EN is introduced before forming ZnS clusters (e.g. scheme C), it leads to the formation of $ZnS(EN)_{0.5}$ NBs (Fig. 3), in which the hybrid nanostructures are interconnected through covalent bonds, forming 3D superlattice structures . The atomic layers in these zinc sulfide slabs are in wurtzite stacking sequences. The slabs are then connected to each other with their (110) facets bonding to the two tip of one EN layer. It is found that the complex precursor forms first at room temperature, and the $ZnS(EN)_{0.5}$ hybrid nanostructure starts to form at 180^{o}C, because only at this temperature can the system reach the phase TTT-EN component.[43]

Conclusions

In our work series ZnS nanostructures including NPs, NWs, $ZnS(EN)_{0.5}$ hybrid NBs, and single-crystal NBs are one-pot synthesized in solvothermal system by using EN as structure-directing and surface-passivating coordination agent. Comprehensive structure characterizations evidence that the modulation effect of EN molecules exhibits distinct manifestations varying from surface stabilizing to internal bridging based on the coordination interaction with Zn atoms. When introduced after the formation of ZnS precursor, EN passivates the none-polarized facets of ZnS clusters (e.g. (100), (110)) and restrains them to nanoscale in those directions, while changing atoms stacking sequences from fcc to hcp and activating the anisotropic growth along the [001] axis of WZ into 1D. In this situation, EN prefers to adjust the crystal growth behavior at lattice scale rather than the assembly manner at nanoscale. On the contrast, when EN is added before ZnS nucleation are formed, EN molecules serve as the bridging blocks and yield layered $ZnS(EN)_{0.5}$ hybrid structure through connection between the two tips of EN molecule and surface atoms in (110)WZ of ZnS slabs. The $ZnS(EN)_{0.5}$ hybrid structure can be flexibly transformed into single-crystal NBs after the removal of EN component. This work provides a general strategy for tuning optical properties of tetrahedrally coordinated materials by controlling their phases and morphologies under precise modulation of organic amine molecules.

Acknowledgements

This work was supported by the National Natural Science Foundation of China (No. 11304209), China Scholarship Council (201506075044), Fundamental Research Funds for the Central Universities (ZYGX2014J035). The JEOL JEM-3100R05 TEM used for this investigation were funded by National Science Foundation Grants (Grant No. DMR-0723032).

Notes and references

1 J. H. Yu, S. H. Kwon, Z. Petrasek, O. K. Park, S. W. Jun, K. Shin, M. Choi, Y. Il Park, K. Park, H. B. Na, N. Lee, D. W. Lee, J. H. Kim, P. Schwille and T. Hyeon, Nat. Mater., 2013, 12, 359-366.
2 L. F. Hu, J. Yan, M. Y. Liao, H. J. Xiang, X. G. Gong, L. D. Zhang and X. S. Fang, Adv. Mater., 2012, 24, 2305-2309.
3 X. J. Xu, L. F. Hu, N. Gao, S. X. Liu, S. Wageh, A. A. Al-Ghamdi, A. Alshahrie and X. S. Fang, Adv. Funct. Mater., 2015, 25, 445-454.
4 Y. F. Yu, J. Zhang, X. Wu, W. W. Zhao and B. Zhang, Angew. Chem. Int. Edit., 2012, 51, 897-900.
5 R. H. Zhou, M. Li, S. L. Wang, P. Wu, L. Wu and X. D. Hou, Nanoscale, 2014, 6, 14319-14325.
6 L. F. Hu, M. M. Brewster, X. J. Xu, C. C. Tang, S. Gradecak and X. S. Fang, Nano Lett., 2013, 13, 1941-1947.
7 H. Liu, L. F. Hu, K. Watanabe, X. H. Hu, B. Dierre, B. Kim, T. Sekiguchi and X. S. Fang, Adv. Funct. Mater., 2013, 23, 3701-3709.
8 T. T. Zhuang, P. Yu, F. J. Fan, L. Wu, X. J. Liu and S. H. Yu, Small, 2014, 10, 1394-1402.
9 S. C. Rai, K. Wang, Y. Ding, J. K. Marmon, M. Bhatt, Y. Zhang, W. L. Zhou and Z. L. Wang, ACS Nano, 2015, 9, 6419-6427.
10 T. T. You, J. L. Wang, H. Feng, K. M. Chen, W. L. Fan, C. Zhang and R. S. Miao, Dalton Transactions, 2013, 42, 7724-7730.
11 D. S. Li, Crystengcomm, 2013, 15, 10631-10637.
12 Z. F. Zhang, J. Li, J. K. Jian, R. Wu, Y. F. Sun, S. F. Wang, Y. S. Ren and J. J. Li, J. Cryst. Growth, 2013, 372, 39-42.
13 A. Fischereder, M. L. Martinez-Ricci, A. Wolosiuk, W. Haas, F. Hofer, G. Trimmel and G. Soler-Illia, Chem. Mat., 2012, 24, 1837-1845.
14 G. Z. Shen, Y. Bando, J. Q. Hu and D. Golberg, Appl. Phys. Lett., 2007, 90, 123101.
15 S. W. Zhang, B. S. Yin, H. Jiang, F. Y. Qu, A. Umar and X. Wu, Dalton Transactions, 2015, 44, 2409-2415.
16 Z. G. Chen, J. Zou, G. Liu, X. D. Yao, F. Li, X. L. Yuan, T. Sekiguchi, G. Q. Lu and H. M. Cheng, Adv. Funct. Mater., 2008, 18, 3063-3069.
17 S. A. Acharya, N. Maheshwari, L. Tatikondewar, A. Kshirsagar and S. K. Kulkarni, Cryst. Growth Des., 2013, 13, 1369-1376.
18 W. T. Yao, S. H. Yu and Q. S. Wu, Adv. Funct. Mater., 2007, 17, 623-631.
19 Q. F. Lu and D. J. Wang, in Functional Materials and Nanotechnology, eds. B. Xu and H. Y. Li, International Materials Research Society, Zhengzhou, PEOPLES R CHINA, 2012, vol. 496, ch. 1, pp. 46-49.
20 S. Sperinck, T. Becker, K. Wright and W. R. Richmond, J. Incl. Phenom. Macrocycl. Chem., 2009, 65, 89-95.
21 X. Y. Huang, H. R. Heulings, V. Le and J. Li, Chem. Mat., 2001, 13, 3754-3759.
22 S. A. Acharya, S. Darulkar and P. Choudhary, in Advanced Nanomaterials and Nanotechnology, eds. P. K. Giri, D. K. Goswami and A. Perumal, Springer Berlin Heidelberg, Guwahati, INDIA, 2013, vol. 143, ch. 6, pp. 65-75.
23 X.Y. Huang, J. Li, Y. Zhang, A. Mascarenhas J. Am. Chem. Soc., 125 (2003), pp. 7049–7055

24 R. M. Wang and W. Liu, Thin Solid Films, 2012, 522, 40-44.
25 W. Liu, R. M. Wang and N. Wang, Appl. Phys. Lett., 2010, 97, 041916.
26 W. Liu, N. Wang, R. M. Wang, S. Kumar, G. S. Duesberg, H. Z. Zhang and K. Sun, Nano Lett., 2011, 11, 2983-2989.
27 X. Ouyang, T. Y. Tsai, D. H. Chen, Q. J. Huang, W. H. Cheng and A. Clearfield, Chem. Commun., 2003, 1107-1107.
28 A. Hernandez-Gordillo, F. Tzompantzi and R. Gomez, Catal. Commun., 2012, 19, 51-55.
29 Z. X. Deng, C. Wang, X. M. Sun and Y. D. Li, Inorg. Chem., 2002, 41, 869-873.
30 X. S. Peng, G. W. Meng, J. Zhang, L. X. Zhao, X. F. Wang, Y. W. Wang and L. D. Zhang, J. Phys. D Appl. Phys., 2001, 34, 3224-3228.
31 N. R. Pawaskar, S. D. Sathaye, M. M. Bhadbhade and K. R. Patil, Mater. Res. Bull., 2002, 37, 1539-1546.
32 C. C. Yang and S. Li, J. Phys. Chem. C, 2008, 112, 2851-2856.
33 W. T. Yao, S. H. Yu, L. Pan, J. Li, Q. S. Wu, L. Zhang and H. Jiang, Small, 2005, 1, 320-325.
34 X. S. Fang, Y. Bando, G. Z. Shen, C. H. Ye, U. K. Gautam, P. Costa, C. Y. Zhi, C. C. Tang and D. Golberg, Adv. Mater., 2007, 19, 2593-2596.
35 J. N. Rebilly, P. W. Gardner, G. R. Darling, J. Bacsa and M. J. Rosseinsky, Inorg. Chem., 2008, 47, 9390-9399.
36 Y. Gao, Z. Y. Zhi, Small, 2011, 7, 2133-2146.
37 Y. S. Xia, T. D. Nguyen, M. Yang, B. Lee, A. Santos, P. Podsiadlo, Z. Y. Tang, S. C. Glotzer, N. A. Kotov, Nature Nanotechnology 2011, 6, (9), 580-587.
38 Y. S. Xia, Z. Y. Tang, Chemical Communications 2012, 48, (51), 6320-6336.
39 J. X. Gong, G. D. Li, Z. Y. Tang, *Nano Toda*y 2012**,** 7, (6), 564-585.
40 C. Lu, Z. Tang, *Advanced Materials 2015,* 10.1002/adma.201502869
41 Z. Y. Tang, N. A. Kotov and M. Giersig, Science, 2002, 297, 237-240.
42 Xiong, Y. S.; Deng, K.; Jia, Y. Y.; He, L. C.; Chang, L.; Zhi, L. J.; Tang, Z. Y. *Small* **2014,** 10, (8), 1523-1528.
43 C. Y. Moon, G. M. Dalpian, Y. Zhang and S. H. Wei, Chem. Mat., 2006, 18, 2805-2809.

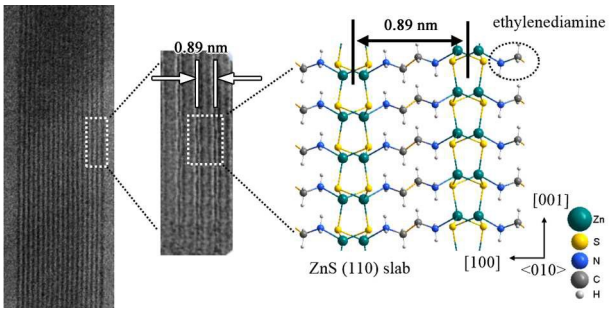

Lateral view of single atomic layered $ZnS(EN)_{0.5}$ hybrid structure (left: BF-STEM image, right: schematic structure).